Dynamic Behavior of Iron Forms in Rapid Reduction of Carbon-Coated Iron Ore

Katsuyasu Sugawara, Koji Morimoto, and Takuo Sugawara
Div. of Materials Process Engineering, Akita University, Akita City, Japan

Joshua S. Dranoff
Dept. of Chemical Engineering, Northwestern University, Evanston, IL 60208

As a part of a fundamental study of the kinetics of rapid smelting reduction of iron oxide with solid carbon, particles of carbon-coated iron ore were prepared by heating a mixture of iron ore and phenolphthalein (a model compound of coal tar) at 773 K in a nitrogen stream. The reduction behavior of the carbon-coated iron ore particles during rapid heating was studied using a drop-tube reactor at temperatures from 1,073 to 1,773 K. The reduction extent increased rapidly with the beginning of melting at temperatures over 1,650 K, reaching 60% at 1,773 within 0.7 s. The observed changes in the distribution of iron states in the particles were successfully simulated.

Introduction

Current steel making using a blast furnace requires the processes of coking high-quality coal and sintering iron ore. Direct reduction of iron ore is separated into gas-based and solid-based processes. The gas-based reduction is limited to ASEAN, the middle east, and Latin America, which have natural-gas resources. Steam-coal-based direct reduction has the potential to produce steel economically on a large scale because of the wide distribution of coal in the world and the depletion of caking coal (Rao, 1974; Fruehan, 1977; Srinivasan and Lahiri, 1977; Abraham et al., 1979; Haque et al., 1993).

The direct iron-ore smelting-reduction process, in which noncaking coal and iron-ore powder can be used directly without coke, is expected to lower costs as well as CO_2 production, and is now attracting a great deal of attention as one of the new iron-making processes for the next century. Development of this process requires an accurate understanding of the reaction mechanism and evaluation of the kinetics under melting conditions. Recently, studies on the preliminary reduction of iron ore utilizing coal volatiles (Usui et al., 1992) and on the reduction of molten iron ore by hydrogen or carbon monoxide have been reported (Hayashi et al., 1994). While several investigations of the reduction rate of liquid iron oxide with solid carbon have been reported (Sato et al., 1987; Kin et al., 1989; Nagasaka and Ban-ya, 1992), most of them were conducted by measuring the CO gas volume generated from iron-oxide pellets thrown into a graphite crucible heated to the desired temperatures. This crucible method suffers from uncertainties in the liquid−solid interface area as a result of intense gas evolution as well as heat-transfer limitations within the pellets. Furthermore, dynamic changes in the distribution of the various forms of iron under such nonisothermal conditions have not been investigated.

In a series of studies on the development of the raceway smelting reduction process in a blast furnace, Nozawa et al. investigated the reduction behavior of iron ore in a mixture of particles of iron ore and coal during rapid heating in a carbon monoxide and carbon dioxide atmosphere. They demonstrated that the solid carbon produced from carbonaceous volatiles during coal pyrolysis was deposited on the surface of the iron particles and subsequently acted as a reducing agent to promote the rate of wustite reduction to metallic iron under melting conditions (Nozawa et al., 1992, 1993a,b). However, there have not been satisfactory quantitative and kinetic interpretations for direct-iron-ore smelting-reduction because of complex reactions that occur at high temperatures and under melting conditions, and which are accompanied by secondary indirect reduction due to gaseous products (Nagasaka and Ban-ya, 1992).

Correspondence concerning this article should be addressed to K. Sugawara.

The objective of the present study was to obtain fundamental data on the rate of reduction of iron-ore particles in solid and melting conditions using solid carbon as a reducing agent. The iron-ore particles with a carbon coating were heated in a nitrogen stream using a drop-tube reactor with furnace temperatures that ranged from 1073 K to 1773 K. Such a reactor has the advantages over the conventional crucible-type reactor of rapid heating without the particles adhering to the reactor wall, which might introduce contaminants, and of the minimum influence of indirect reduction by gaseous products. Sequential changes were observed in the distribution of the iron forms present during treatment times ranging from 0.2 s to 0.7 s, which were effected by changing the length of the heating section. The nonisothermal dynamics of reduction from hematite to metallic iron were simulated by solving the momentum, heat, and material balances for a particle of iron-ore falling freely in the reactor.

Experimental Studies

The iron ore used in this study was Australian Hamersley containing 64.6 wt. % of total iron, composed of 92.2 wt. % of Fe_2O_3 and 0.15 wt. % of FeO crushed and sieved to $-200+250$ mesh. Phenolphthalein was selected as the carbonaceous material to be used to cover the particle surface of the iron-ore particles because of its thermal plasticity and because the smaller molecular-weight compounds, anthracene and naphthalene, did not produce sufficient carbon deposits on the iron particles. A mixture of iron-ore particles and phenolphthalein (Nakarai Tesuku Co. Ltd., GR grade) was heated in an alumina crucible with an infrared gold image furnace (Ulvac-Sinku Riko) under nitrogen at 20 K/min up to 773 K. A temperature higher than 673 K and a holding time of 10 minutes at the final temperature were necessary to obtain a sufficient amount of carbon deposited on the iron particle. When all of the iron ore consists of hematite, the mixture should contain 18.4 wt. % carbon for direct reduction of hematite to metallic iron according to the following equation: $Fe_2O_3+3C \rightarrow 2Fe+3CO$. While the amount of carbon coated on the iron particle was found to increase linearly with the amount of phenolphthalein in the mixture, a carbon-coated iron ore, containing 29 wt. % carbon, was used in this study. This ore was prepared by mixing phenolphthalein and iron-oxide ore in a 1-to-1 weight ratio (Sugawara et al., 1996).

Figure 1 shows the drop-tube reactor. The reactor was an alumina tube with a 28 mm ID and an overall length of 105 cm, divided into sections of 25, 40 and 40 cm. Reactor temperature was controlled by three sequential electric furnaces. Iron-ore particles were supplied from the hopper into the reactor at a feed rate of 10 g/h. Nitrogen gas flowed downwards at 600 cc-NTP/min from the gas inlet. The length of time the sample particle remained in the reactive zone was modified by changing the length of the heating section (by switching the electric furnaces on or off in sequence from the top of reactor). The initial nonisothermal temperature profile in the reactor made it possible to obtain data for nonisothermal kinetic analysis.

Average particle size was determined by image analysis with a microscope (Nikon Optiphoto). Apparent particle density was measured with a pycnometer (JIS M8717). Analysis of

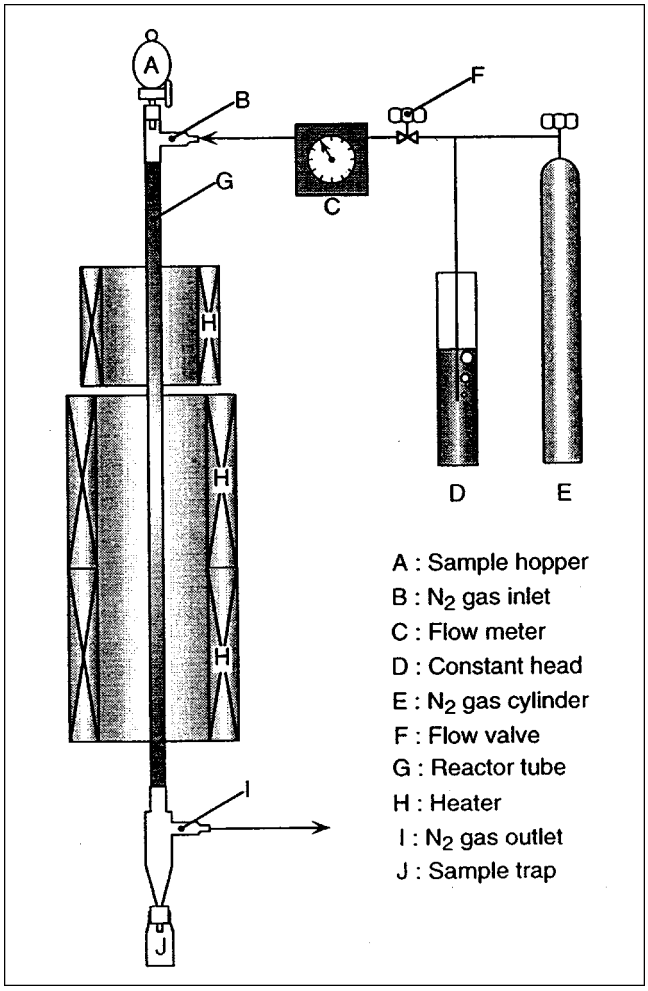

Figure 1. Drop-tube reactor.

total iron, wustite, and metallic iron content of the iron-ore particles was done according to standard methods (JIS M8812 and M8713). The sample was dissolved in hot hydrochloric acid in the presence of tin chloride. Residue was dissolved in hydrofluoric acid with potassium sulfide and then mixed with the solution just cited. All of the trivalent iron was reduced to bivalent iron with tin chloride. The total amount of iron in the sample was determined from bivalent iron in the solution, which could be measured by oxidation-reduction titration with potassium chromate.

Metallic iron is dissolved in a bromine–methanol solution, but bivalent iron is not. The amount of metallic iron was determined by EDTA titration after oxidation with presulfuric ammonium. The residue in the bromine–methanol solution was dissolved in hydrochloric acid. The amount of wustite was determined from the bivalent iron in this solution. The carbon content of the coated ore was measured using a Horiba EMIA-1200 infrared spectrometer with high-frequency induction heating. The principle of the method by EMIA-1200 is that a sample is combusted with tungsten, tin, and iron particles as promoters by high-frequency induction heating under oxygen, and that CO_2 and CO are analyzed quantitatively by an infrared analyzer.

Results and Discussion

Solid–solid reduction

The first section of experiments was carried out below the melting temperature of the ore particles. Figure 2 shows the measured change in the extent of reduction with the distance from the sample hopper for carbon-coated iron-ore particles as well as the corresponding reactor-wall temperature distributions. The three furnaces were controlled independently to maintain the desired temperature distribution in the reactor. The data denoted by case A were obtained with temperatures of 1,073 K, 1,273 K, and 1,273 K for furnaces I, II, and III, respectively, from the top of the reactor (furnace I acted primarily as a preheater for the particles and the nitrogen gas). The extent of reduction was defined as: {1−(oxygen content after reduction/oxygen content before reduction)}× 100 [%], where the oxygen content before and after reduction was determined from the amount of iron forms (Fe_2O_3, FeO, and Fe). These reduction experiments were carried out using maximum furnace temperatures of 1,273 K and 1,573 K, which were under the melting point of wustite (1,650 K). The extent of reduction clearly increased with reactor temperature and distance from the sample hopper. Amounts of reduction of 23% and 38% were obtained at the maximum furnace temperatures of 1,273 K (case A) and 1,573 K (case B).

A change in the makeup of Fe, Fe(II), and Fe(III) with distance from the sample hopper is shown for cases A and B in Figure 3. In case A, Fe(II) appeared first at 74 cm, and then metallic iron was produced at 116 cm. While only 8% of metallic iron was obtained at 146 cm under the conditions of case A, this experiment demonstrated that the reduction of carbon-coated iron ore progressed with coexistence of Fe, Fe(II), and Fe(III) during the rapid heating. Figure 3 indicates that the amount of metallic iron reached 20% at 146 cm at the maximum temperature of 1573 K (case B).

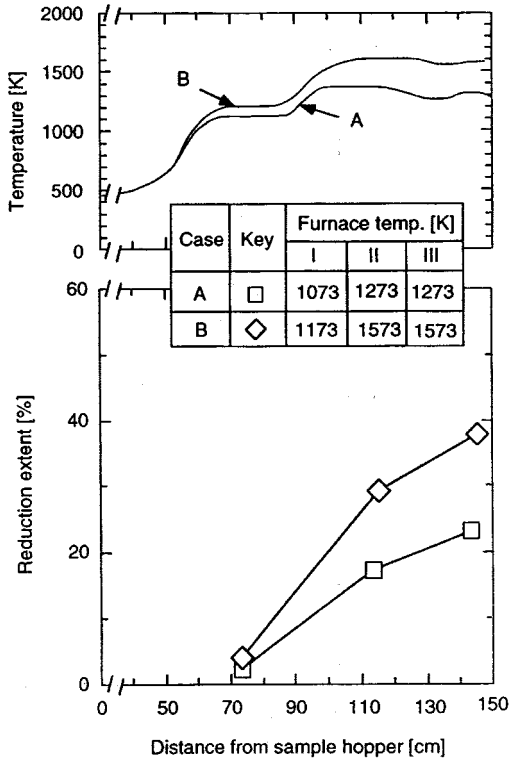

Figure 2. Changes in reduction extent and reactor-wall temperature with distance from sample hopper for cases A and B.

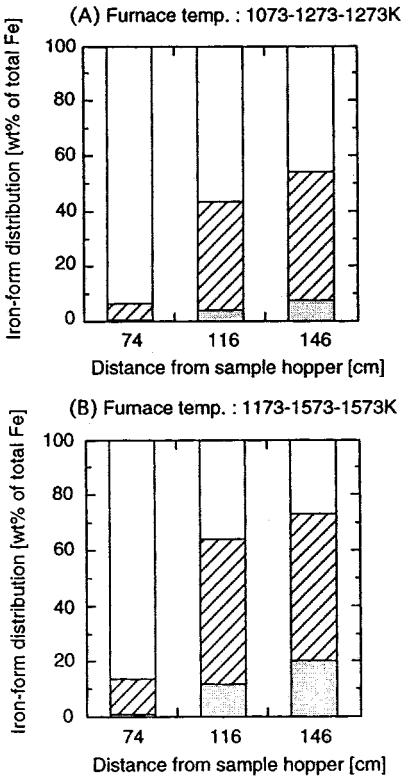

Figure 3. Change in iron-form distribution with distance from sample hopper and furnace temperature for cases A and B: □ = Fe (III); ▨ = Fe (II); ■ = Fe.

As was pointed out earlier, the length of the heated section of the drop tube was changed by switching the power to the three furnace sections. It was observed in preliminary experiments, and later verified by simulations, that the furnace temperature began to fall before the end of the last heated section, as which point the particles began to cool. Therefore, as a first approximation, it was assumed that the reduction reactions stopped once a particle entered the cooling zone. The measured extent of reduction data was then plotted against the distances where the cooling zone began in each case (at 74, 116, and 146 cm from the sample hopper).

Smelting reduction

Experiments were then conducted at maximum reactor temperatures of 1650 and 1773 K, in cases C and D, respectively. A study of scanning electromicrographs confirmed partial melting of sample particles in case C. Figure 4 shows SEM photographs of carbon-coated iron ore before and after rapid heating. Particles obtained in case D were round, indicating that most of the particles were melted while flowing through the heating section at the highest temperature. Changes in the extent of reduction and reactor temperature distribution with distance from the sample hopper for these

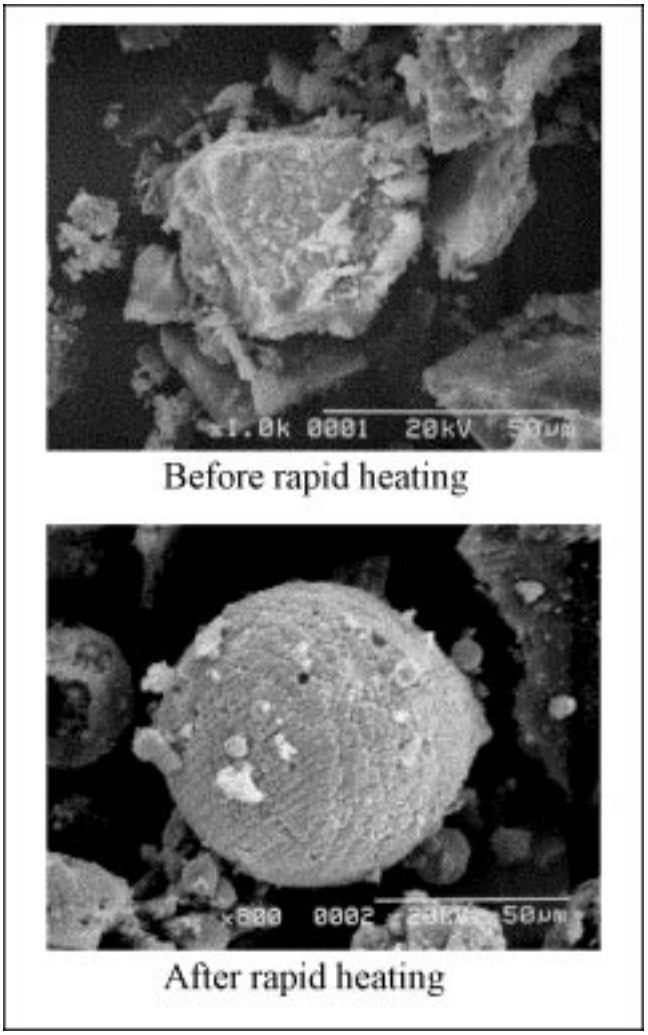

Figure 4. SEM photograph of typical carbon-coated iron-ore particles before and after rapid heating (case D).

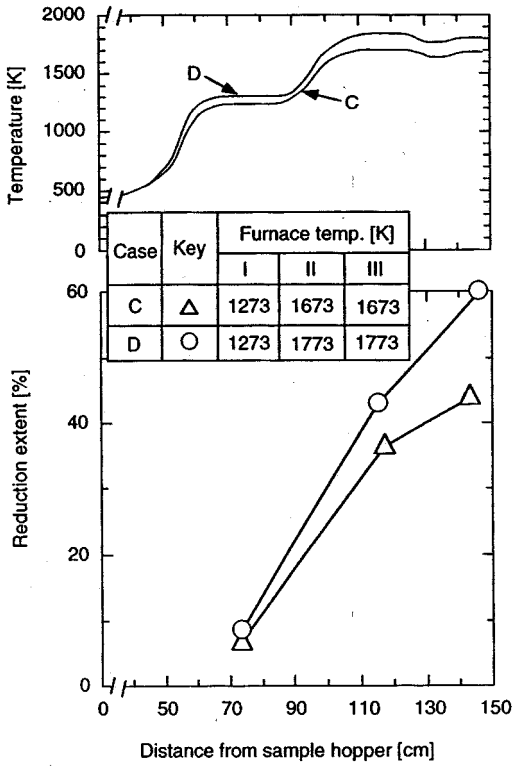

Figure 5. Changes in reduction extent and reactor-wall temperature with distance from sample hopper for cases C and D.

cases are shown in Figure 5. The extent of the reduction of the iron ore increased rapidly with the furnace temperature and reached 60% in case D. The distribution of iron states shown in Figure 6 indicates that the content of metallic iron increased with increases in heating length and furnace temperature, as expected. These observations suggest that the reduction rate of iron-ore particles began to increase rapidly with the onset of particle melting. The reduction, particularly from wustite to metallic iron, was accelerated, which implies that melting wustite can contact the surface carbon more easily than solid iron oxide. Metallic iron cores or nuclei were also observed within the wustite shell, which might be explained as the effects of surface tension (Nozawa et al., 1992).

Modeling the reduction process

A model for the progress of the reduction reactions has been generated based on momentum, energy, and mass balances applied to a moving particle. It was first assumed that the iron-ore particles fall freely from the sample hopper to the horizontal cross section of the reactor tube, where they encounter the downward laminar flow of nitrogen gas. The momentum equation of a particle is as follows:

$$dv_P/dt = -(3/4)(\rho_G/\rho_P D_P) C_{DP}(v_P - u_G)^2 + (1 - \rho_G/\rho_P) g, \quad (1)$$

where v_P and u_G are the velocity of falling particles and the average velocity of nitrogen gas, respectively; D_P is the average particle diameter; and ρ_P and ρ_G are apparent density of particle and nitrogen gas, respectively. The drag coefficient, C_{DP}, is given in Eqs. 2 and 3 as a function of the particle Reynolds number, Re_P, calculated by Eq. 4:

$$C_{DP} = 24/Re_P \qquad (Re_P < 2) \quad (2)$$

$$C_{DP} = 10/(Re_P)^{0.5} \qquad (2 \leqq Re_P < 25) \quad (3)$$

$$Re_P = D_P(v_P - u_G)\rho_G/\mu_G, \quad (4)$$

where μ_G is the viscosity of nitrogen gas. The change in measured particle diameter and apparent density with heat treatment in the furnace could be expressed as a polynomial function of L, the distance from the top of the furnace, assuming that there was negligible change during particle cooling:

$$\rho_P = a_0 + a_i L + a_2 L^2 + a_3 L^3. \quad (5)$$

Coefficients a_0 through a_3 are listed in Table 1. Figure 7 shows how the apparent particle density changed with the distance from the sample hopper under different heating his-

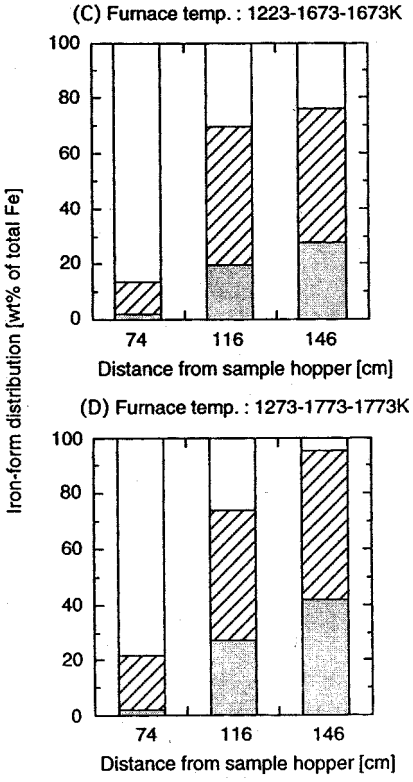

Figure 6. Change in iron-form distribution with distance from sample hopper and furnace temperature for cases C and D: □ = Fe (III); ▨ = (II); ■ = Fe.

tories. The density increased with the distance and with the maximum furnace temperature, or equivalently, as reduction of the iron ore progressed. On the other hand, no appreciable change in the average particle diameter was observed after the rapid heating.

The energy-conservation equation for a sample particle is expressed by the following equation:

$$dT_p/dt = \left[\pi D_p^2\left\{h_c(T_G - T_P) - \sigma\epsilon\left(T_w^4 - T_P^4\right)\right\} - \Delta H\right]/C_{PT}, \tag{6}$$

where T_P, T_G, and T_W are particle, gas, and reactor wall temperatures, respectively; σ and ϵ are Boltzmann's constant and emissivity. The film coefficient of heat transfer, *hc*, is given by Eq. 7

$$h_c = (k_G/D_P)\left(2.0 + 0.6\,Re_p^{0.5}Pr^{0.33}\right), \tag{7}$$

where *Pr* is Prandtl number represented by Eq. 8:

Table 1. Coefficients in Eq. 5

Case	Furnace Temp. [K]	a_0	a_1	a_2	a_3
A	1,073–1,273–1,273	5.36	−0.127	1.51×10^{-3}	-5.03×10^{-6}
B	1,173–1,573–1,573	7.15	−0.20	2.43×10^{-3}	-8.37×10^{-6}
C	1,223–1,673–1,673	4.37	−0.10	1.36×10^{-3}	-4.80×10^{-6}
D	1,273–1,773–1,773	2.64	−0.047	9.36×10^{-4}	-3.77×10^{-6}

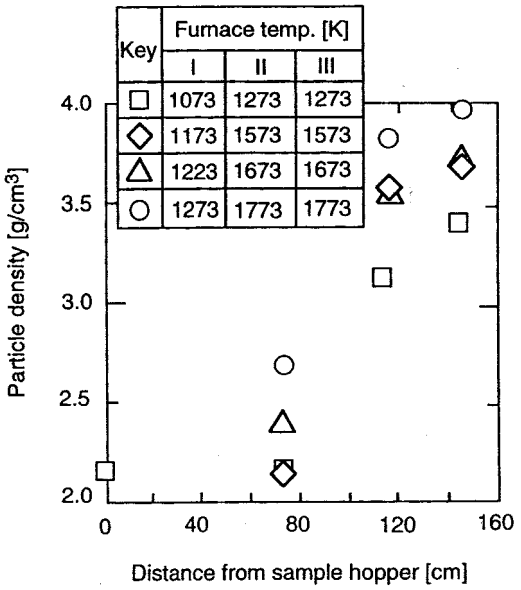

Figure 7. Change in apparent particle density with distance from sample hopper and furnace temperature.

$$Pr = C_{PG}\,\mu_G/k_G. \tag{8}$$

The emissivity of carbon-coated iron ore was taken to be 0.9. The heat capacity of the solid particle C_{PT} was calculated as a mass-averaged value of the heat capacities of the three forms of iron as well as carbon (contribution of other trace components being neglected):

$$C_{PT} = \Sigma C_{pi}\cdot W_i$$
$$(i = 1 \text{ to } 4;\ 1{:}Fe_2O_3;\ 2{:}FeO;\ 3{:}Fe,\ 4{:}\text{ carbon}), \tag{9}$$

where W_i is the weight fraction of each component (from 1 to 4). It was also assumed that the temperature distribution within a particle was uniform because of the very small particle size and the large thermal conductivity of the iron-ore particles.

The energy-conservation equation for nitrogen gas, neglecting the relatively small amount of heat transferred to the particles, is shown below:

$$dT_G/dx = (4h_G/\rho_G u_G C_{PG} D_r)(T_w - T_G). \tag{10}$$

The solution of this equation will yield the nitrogen gas temperature-distance profile, which is independent of the solid particles. Note that for convenience, the distance variable may be related directly to the residence time of the falling particles. The film coefficient of heat transfer, h_G, was calculated from Eq. 11:

$$h_G = 1.86\,(Re_G PrD_r/x)^{0.33}(\mu_G/\mu_W)^{0.14}(k_G/D_r) \tag{11}$$

$$Re_G = D_r u_G \rho_G/\mu_G, \tag{12}$$

where *Pr* and Re_G are the gas-phase Prandtl and Reynolds numbers, D_r is diameter of the reactor tube, and x and μ_w

are respectively, the distance from the gas inlet and the gas viscosity at the reactor-wall temperature.

The reduction of the carbon-coated iron ore is assumed to progress according to the following sequence:

$$Fe_2O_3(s) + C \rightarrow 2FeO(s) + CO \tag{13}$$

$$FeO(s) + C \rightarrow Fe(s) + CO \qquad (T_P < 1{,}650\ \text{K}) \tag{14}$$

$$FeO(l) + C \rightarrow Fe(l) + CO \qquad (T_P \geqq 1{,}650\ \text{K}). \tag{15}$$

It has been reported that the reduction of the iron ore progresses topochemically in the solid state below the melting point of wustite, and metallic iron core was observed within the wustite shell during the smelting reduction. Since coexistence of Fe(III), Fe(II), and Fe complicates the reaction mechanism under the experimental conditions studied, a volume-reaction model was applied to analyze the reaction kinetics to avoid such a complication. It is assumed that reaction rates may be expressed by following first-order kinetic model equations:

$$r_{Fe_2O_3} = -k_1[Fe_2O_3] \tag{16}$$

$$r_{FeO(s)} = 2k_1[Fe_2O_3] - k_2[FeO(s)] \qquad (T_P < 1{,}650\ \text{K}) \tag{17}$$

$$r_{FeO(l)} = 2k_1[Fe_2O_3] - k_3[FeO(l)] \qquad (T_P \geqq 1{,}650\ \text{K}) \tag{18}$$

$$r_{Fe(s\ or\ 1)} = k_2[FeO(s)] + k_3[FeO(l)]. \tag{19}$$

An Arrhenius-type temperature dependency was also assumed for the rate constants in this study.

$$k_i = k_{i0} \exp(-E_i/RT) \qquad (i = 1 \text{ to } 3). \tag{20}$$

Total heat of reaction in Eq. 6 was calculated by Eq. 21

$$\Delta H_T = \Delta H_l \cdot r_{Fe_2O_3} + \Delta H_2 \cdot r_{FeO(s)} + \Delta H_3 \cdot r_{FeO(l)}, \tag{21}$$

where ΔH_1, ΔH_2, and ΔH_3 are the heats of reaction corresponding to Eqs. 13, 14, and 15. Heat of melting for wustite was neglected for the estimation in Eq. 21 because of its small value.

The simultaneous momentum, heat, and material balances in Eqs. 1 through 12 and Eqs. 16 through 21 were solved by means of the Runge–Kutta–Gill algorithm. The frequency factors and activation energies indicated in Eq. 20 were considered to be adjustable parameters and were optimized to fit the experimental results. Figure 8 shows the experimental results and simulated curves for the distribution of the various forms of iron obtained for furnace temperatures of 1,073 K–1,273 K–1,273 K (corresponding to case A) as functions of the estimated particle residence time (or length) in the reactor. The experimental profile of the reactor-wall temperature and the calculated particle temperature are also shown in the figure. The solid lines in Figure 8 indicate the simulated changes in the distribution of iron forms. As shown, the experimental results were simulated successfully using the following values for the kinetic parameters: $k_{10} = 600\ s^{-1}$, $k_{20} = 1{,}300\ s^{-1}$, $E_1 = 12\ \text{kcal} \cdot \text{mol}^{-1}$, and $E_2 = 18\ \text{kcal} \cdot \text{mol}^{-1}$ for the reduction at temperatures below the melting point of wustite. The experimental results and simulated curves for iron-form distribution obtained for case D at high furnace temperatures (1,273 K–1,773 K–1,773 K) are shown in Figure 9. Kinetic parameters for the reduction of liquid wustite to metallic iron were evaluated to be $k_{30} = 3{,}400\ s^{-1}$ and $E_3 = 21\ \text{kcal} \cdot \text{mol}^{-1}$; the parameters for the other two reactions were as determined earlier. It can be seen that the reduction from wustite to metallic iron is accelerated by temperatures greater than the melting point of wustite. The variation of emissivity between plus or minus 0.1 does not have an appreciable influence on the kinetic parameters, but the activation energies increase by 1.0 kcal/mol when the heats of reaction are not considered.

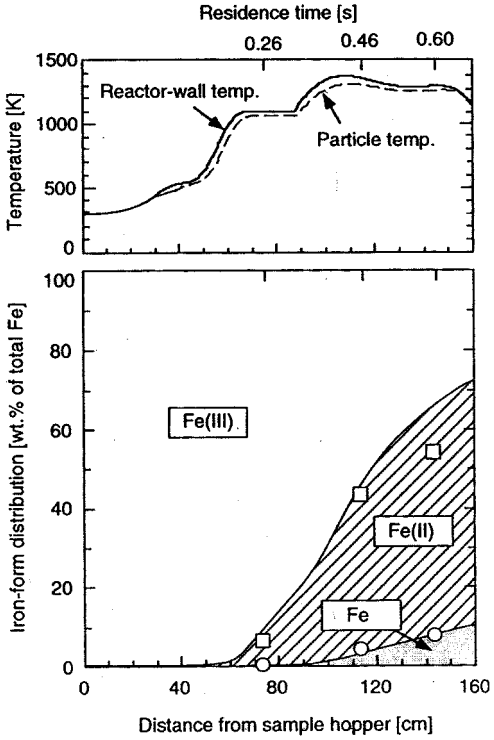

Figure 8. Simulated curves and experimental results for iron-form distribution with temperatures for case A.

Previous works have reported that the reduction rate of pure molten iron oxide depended on the reducing agent in the order of H_2 > Fe–C melt (carbon in molten iron) > solid carbon > CO gas, and that the smelting reduction rate was one order of magnitude larger than the solid-state reduction by H_2 and CO gases (Nagasaka et al., 1992). The reduction rates proposed in earlier studies were expressed in the units of [mol-CO/cm^2·s] and [mol-FeO/cm^3·s] because they were evaluated from the amount of CO gas evolved from molten iron oxide using a graphite crucible or graphite rod as reducing agents; however, those analyses involved uncertainties in the interfacial area between solid carbon and iron oxide and the large difference in volume of iron oxide per interfacial area. According to the study by Sato et al. (1987), the reduc-

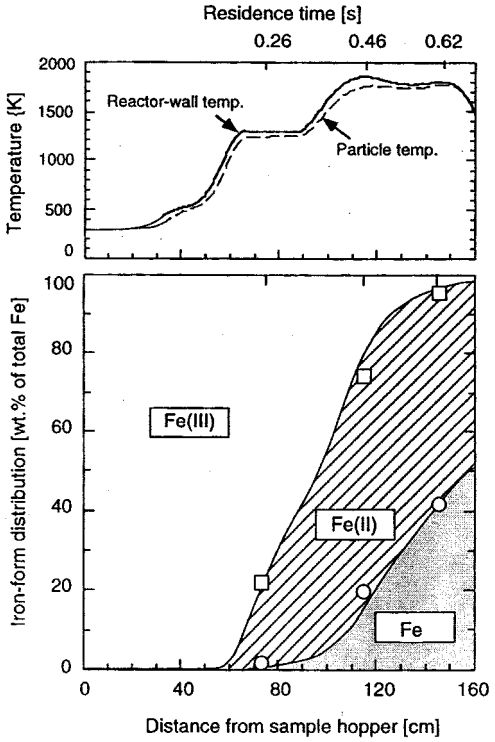

Figure 9. Simulated curves and experimental results for iron-form distribution with temperatures for case D.

tion rate of molten iron oxide by solid carbon was 2.1×10^{-5} to 8.2×10^{-5} [mol-FeO/cm^2·s] for temperatures between 1693 and 1893 K with a graphite rod in an alumina crucible. In order to compare the present results, the values of k_3[FeO]/S were evaluated as 8.3×10^{-4} to 1.6×10^{-3} [mol-FeO/cm^2·s] in the preceding temperature range using the kinetic constant k_3 reported previously, the surface area S of an iron particle, and the FeO content in a particle used in the present study. The rates calculated were 20 to 40 times larger than Sato's results. The relatively large reduction rate in this study may have resulted from the different properties of the amorphous carbon compared to the graphite crucible, such as reactivity and wettability by liquid iron oxide. Furthermore, the large interface between solid carbon and iron oxide per iron oxide volume and the small diffusion distance of wustite and metallic iron within the small iron-oxide particle might also influence the large reduction rate. Lloyd et al. (1975) gave a reduction rate of 7.9×10^{-4} to 5.0×10^{-3} [mol-FeO/cm^2·s] for the Fe–C melt system, which is close to the reduction rates found in this study. Formation of a Fe–C melt system by the partial dissolution of carbon into molten iron oxide might also be responsible for the large reduction rate of the present study.

Conclusion

The rapid smelting reduction of carbon-coated iron-ore particles has been successfully carried out in a drop-tube reactor. Dynamic changes in the state of the iron were followed by varying the length of the reactor heating section and the temperature distribution (from 1,073 K to 1,773 K). The results show that Fe, Fe(II), and Fe(III) coexisted during reduction, and the reduction from wustite to metallic iron appeared to accelerate with temperatures above the melting point of wustite. The change in the form of the iron was successfully simulated by solving the simultaneous momentum, heat, and material balances for a falling particle in the drop-tube reactor. The kinetic parameters determined indicated that the reduction rates of liquid wustite by solid carbon is larger than the previously reported values.

Acknowledgments

This work was supported by a Grant-in-Aid for Scientific Research (C) of The Ministry of Education, Science, Sports and Culture, Japan (No. 08650904). The authors thank Mr. T. Sato and Miss. K. Haga for their assistance.

Literature Cited

Abraham, M. C., and A. Ghosh, "Kinetics of Reduction of Iron Oxide by Carbon," *Ironmaking Steelmaking*, **1**, 14 (1979).

Fruehan, R. J., "The Rate of Reduction of Iron Oxides by Carbon," *Metall. Trans. B*, **8B**, 279 (1977).

Hayashi, S., M. Abe, K. Murayama, and Y. Iguchi, "Influence of Gangue Species on Hydrogen Reduction Rate of Liquid Wustite in Gas-Conveyed System," *Curr. Adv. Mater. Process.*, **7**, 82 (1994).

Haque, R., H. S. Ray, and A. Mukherjee, "Reduction of Iron Ore Fines by Coal Fines in a Packed Bed and Fluidized Bed Apparatus —A Comparative Study," *Metall. Trans. B*, **24B**, 511 (1992).

Kim, W. M., G. Granzdorffer, and H. A. Fine, "The Kinetics of Reduction of Iron Oxide from Molten Slag," *Steel Res.*, **60**, 166 (1989).

Lloyd, G. W., D. R. Young, and L. A. Baker, "Reaction of Iron Oxide with Iron-Carbon Melts," *Ironmaking Steelmaking*, **2**, 49 (1975).

Natgasaka, T., and S. Ban-ya, "Rate of Reduction of Liquid Iron Oxide," *Tetsu-to-Hagane*, **78**, 1753 (1992).

Nozawa, K., M. Shimizu, and S. Inaba, "In-Flight Reduction of Fine-Ores in a Hot Reducing Gas Flow," *Tetsu-to-Hagane*, **79**, 443 (1992).

Nozawa, K., K. Shibata, M. Shimizu, and H. Gudenau, "Raceway Smelting Process with Fine Iron Ore Injection from Blast Furnace Tuyers," *Tetsu-to-Hagane*, **79**, 1151 (1993a).

Nozawa, K., K. Shibata, S. Sasahara and M. Shimizu, "Rapid In-Flight Reduction of Fine Ore Injected into a Blast Furnace," *Ironmaking Conf. Proc.*, p. 383 (1993b).

Rao, Y. K., "A Physico-Chemical Model for Reactions between Particulate Solids Occurring through Gaseous Intermediates: I. Reduction of Hermatite by Carbon," *Chem. Eng. Sci.*, **29**, 1435 (1974).

Sato, A., G. Aragane, K. Kamihara, and S. Yoshimatsu, "Reduction Rate of Molten Iron Oxide by the Solid Carbon or the Carbon in Molten Iron," *Tetsu-to-Hagane*, **73**, 812 (1987).

Srinivasan, N. S., and A. K. Lahiri, "Studies on the Reduction of Hematite by Carbon," *Metall. Trans. B*, **8B**, 175 (1977).

Sugawara, K., K. Fukase, and T. Sugawara, "Reduction of Carbon-Coated-Iron Ore in a Drop-Tube Reactor," *Kagaku Kogaku Ronbunshu*, **22**, 969 (1996).

Usui, T., T. Yokoyama, S. Nakahashi, and Z. Morita, "Influence of Processing Temperature Upon the Reduction of Iron Oxide with Coal Carbonization Gas," *Curr. Adv. Mater. Process*, **5**, 172 (1992).

Manuscript received July 7, 1998, and revision received Dec. 14, 1998.